WAVELET MODULATION PERFORMANCE IN FADING CHANNELS

L. Morgoş[*], R. Reiz[*] , C. Gordan[*]
[*]Department of Electronics,
University of Oradea, Faculty of Electrical Engineering and Information Technology,
1 Universităţii St., 410087, Oradea, Romania, E-Mail:lmorgos@uoradea.ro

Abstract –Wavelet modulation simultaneously sends data at multiple rates through an unknown channel. Preuious research has demonstrated that wauelet modulation bit error rate performance in the additive, white, Gaussian noise channel is comparable to theoretical binary phase shift keying. In this paper we extend the inwstigation to the performance of wauelet modulation in several time varying channels: Rayleigh, flat, slow fading channels and frequency selective, slow fading channels.

I. INTRODUCTION

Wavelet modulation has a novel multirate diversity strategy that offers improved message recovery over conventional modulation techniques: if the rnessage is not received at one rate due to channel disturbances, it can be received at another rate where the channel is clear. Wornell and Oppenh& n proposed fractal modulation and analytically calculated its performance in an additive, white, Gaussian noise (AWGN) channel [1]. Ptasinski and Fellman illustrated Wornell and Oppenheim's observation that bit error rate (BER) performance of one-scale wavelet demodulation and binary phase shift keying (BPSK) were identical 121. In this paper we examine the performance of wavelet modulation (WM) in time varying channels. Results for Rayleigh flat fading channels and frequency selective channels are compared to the AWGN channel and to the expected performance of BPSK in a flat fading channel. We evaluate WM performance in the context of military and cellular communication applications; thus, our results shed light on the suitability of wavelet modulation as a technique for signal transmission in a mobile environment.

Section 2 presents an overview of the discrete wavelet transform and wavelet modulation. Section 3 describes the pertinent implementation issues and the channel models. Section 4 depicts the performance of wavelet modulation in the AWGN, flat fading and frequency selective channels. Our conclusions are highlighted in Section 5.

II. DWT & WAVELET MODULATION

The discrete wavelet transform (DWT) of a signal s(t) is given by

$$s_n^m = \int_{-\infty}^{+\infty} s(t) 2^{m/2} \psi\left(2^m t - n\right) dt \qquad (1)$$

$$s(t) = \int_{-\infty}^{+\infty} \sum_{m=-\infty}^{+\infty} \sum_{n=-\infty}^{+\infty} s_n^m 2^{m/2} \psi\left(2^m t - n\right) \qquad (2)$$

where $\psi(t)$ is the wavelet function [3]. Equation (1) represents the DWT and the SF are called the wavelet coefficients; equation (2) is the inverse discrete wavelet transform (IDWT). (Associated with $\psi(t)$ is a corresponding scaling function, $\phi(t)$, and scaling coefficients, a_n^m. Mallat's fast wavelet transform (FWT) provides a computationally efficient, practical, discrete time algorithm for computing the DWT 131. The scaling and wavelet coefficients at scale m can be computed from the scaling coefficients at the next finer scale *m+1* using

$$a_n^m = \sum_l h[l - 2n] a_l^{m+1} \qquad (3)$$

$$s_n^m = \sum_l g[l - 2n] a_l^{m+1} \qquad (4)$$

where *h[n]* and *g[n]* are the lowpass and highpass filters in the associated a-channel analysis filter bank. Equations (3)-(4) represent the FWT for computing the DWT (1). Conversely, it is possible to reconstruct the scaling coefficients a_n^{m+1} by

$$a_n^{m+1} = \sum_l h[2l - n] a_l^m + g[2l - n] s_l^m \qquad (5)$$

Equation (5) represents the IFWT for computing the IDWT; it corresponds to the 2-channel synthesis filter bank.

The wavelet modulated signal to be transmitted, *s(t)*, can be generated via

$$s(t) = \sum_{m=-\infty}^{+\infty} \sum_{n=-\infty}^{+\infty} x[n] 2^{m/2} \psi\left(2^m t - n\right) \qquad (6)$$

where *x[n]* is the data that is modulated onto the wavelet at different scales. In a practical system *x[n]* is modulated onto a finite number of contiguous, octave-width frequency

bands (i.e. $m \in M$ where M is a finite set of contiguous integers).

III. METHODOLOGY

The data to be transmitted takes on one of two equally likely values

$$x[n] \in \left\{ + \sqrt{E_b}, -\sqrt{E_b} \right\} \qquad (7)$$

where E_b is the energy per bit. The wavelet coefficients of $s(t)$ correspond to the data $x[n]$. Thus, $x[n]$ is used in place of s_l^m in (5) to obtain the approximation of $s(t)$ at scale $m + 1$. The data to be modulated at the first scale (scale 10), is given by the vector $x_1^{10} = [x] = [x[0], x[1],.....x[1023]]$. Twice the amount of data is required for modulation at the next higher scale. A periodic replication of the data results in $[xx] = [x] = [x[0], x[1],.....x[1023], x[0], x[1],.....x[1023]]$ .Then a_n^{12} -the approximation of $s(t)$ at scale 12- is obtained via (5). Two wavelets are employed in the simulations: the Daubechies $N = 4$ wavelet and the Daubechies $N = 8$ wavelet. Both are orthogonal, compactly supported wavelets. The $N = 8$ wavelet has 8 vanishing moments and a support length of 15; the $N = 4$ wavelet has 4 vanishing moments and a support length of 7.

In the AWGN channel, zero-mean white Gaussian noise is added to the transmitted signal $s(t)$, so that the received signal $r(t)$ can be represented as

$$r(t) = s(t) + n(t) \qquad (8)$$

where $n(t)$ is a zero-mean white Gaussian noise process with power $N_0 / 2$

Small scale fading is comprised of two independent mechanisms: the time spreading of the signal and the time varying behavior of the channel. A doppler shift causes the time varying behavior of the channel. In our WM experiments, we employed two doppler shifts. For military communications, frequency allocations are in the 900MHz range; assuming a vehicle speed of 45mph, the doppler shift is f_d = 6OHz. For cellular communications, a carrier frequency of f_c = 1800MHz, and a vehicle speed of 45mph results in a doppler shift of f_d = 120Hz

In a slow fading channel the symbol period of the signal is much smaller than the coherence time of the channel $T_s \ll T_c$ [4]. In our WM trials, the longest symbol period occurs at the coarsest scale (scale lo), T_s = 0.977ms. This value is much smaller than the coherence time given by T_c=7.05ms for f_d = 6OHz and T_c = 3.5ms for f_d = 120ms. Hence, the models described in Sections 3.1.3 and 3.1.4 are slow fading channels.

The time dispersion in a multipath environment causes the signal to undergo either flat or frequency selective fading. If the channel has a constant gain and linear phase response over a bandwidth that is greater than the bandwidth of the transmitted signal, then the received signal undergoes flat fading. In a flat fading channel T_s is much larger than the root-mean-square (rms) delay spread

of the channel, σ_τ. In our WM trials T_s at scale 10 is 0.977ms and T_s at scale 13 is $122\mu s$. The form of our simulated model, (9), results in a flat fading channel for all scales (i.e. $\sigma_\tau \ll T_{S13} < T_{S10}$).

Small scale fading can be modeled as a Rayleigh distribution [4, 5]. The received signal is given by

$$r(t) = s(t)ray(t) + n(t) \qquad (9)$$

As in the AWGN channel, $s(t)$ is the transmitted signal and $n(t)$ represents Gaussian noise (it also still dictates the SNR). The impact of the Rayleigh, flat, slow fading channel is given by the multiplicative $ray(t)$; it is coherently demodulated and perfect carrier synchronization is assumed at the receiver.

Frequency selective fading is caused by multipath delays which approach or exceed the symbol period of the transmitted symbol (i.e. $T_S < \sigma_\tau$). In practice, . $T_S \leq 10\sigma_\tau$, will result in a frequency selective channel- the channel introduces intersymbol interference (ISI).
We employed a two ray channel model with an rms delay spread of. $\sigma_\tau = 15{,}3\mu s$; this is comparable to the symbol period at scale 13 (i.e. $T_{S13} = 122\mu s$). For the frequency selective fading channel, the received signal is given by

$$r(t) = \alpha_0 ray_0(t)s(t) + \alpha_1 ray_1(t)s(t - \tau) + n(t) \quad \text{where}$$

$\alpha_0 = 0.707$ and $\alpha_1 = 0.707$ and $\tau = 0.25 T_{S13}$, $ray_0(t)$ and $ray_1(t)$ have Rayleigh distributed amplitudes and uniform phase distributions over $[0, 2\pi)$. The signal energy in the first term and the power of the noise term $n(t)$ determine the SNR of the signal. The sum of $E\{\alpha_0^2 ray_0(t)^2\}$ and $E\{\alpha_1^2 ray_1(t)^2\}$ is set to unity, so that the channel has an average gain of unity.

IV. RESULTS

The digital data sequence is generated using equation (7) with E_b=1. WM BER performance as a function of SNR (given by E_b/N_0) is examined for 5 channels: AWGN; Rayleigh flat fading ($f_d = 60Hz$ and $f_d = 120Hz$); and, frequency selective fading ($f_d = 60Hz$ and $f_d = 120Hz$). Both the flat and frequency selective fading channels are slow fading channels. Demodulation at a particular scale utilizes only 1 copy of the received data at that scale; we assume that all copies are similar. Our BER results are the average of 8 to 10 independent trials. Both the Daubechies $N = 4$ and $N = 8$ wavelets were used.

Figure 1 compares the performance of the Daubechies $N = 4$ and $N = 8$ wavelets in a flat fading channel with a doppler spread of 60Hz. There is no appreciable performance difference between scales 10 and 11 with the $N = 8$ wavelet; thus, the support size does not appear to be important. Results obtained using the Daubechies $N = 4$ did not vary appreciably from the results obtained using the $N = 8$ wavelet for the other channels (even at higher SNRs).
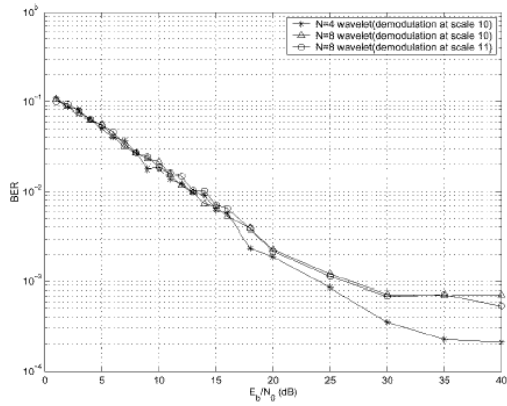
216

Figure1: Bit Error Rate (BER) vs. E_b/N_0 for 2 different wavelets in a flat fading channel with doppler spread 60Hz.

Figure 2 compares the performance of wavelet modulation with that of theoretical BPSK modulation in an AWGN channel. This figure indicates that the performance of WM matches BPSK in an AWGN channel (for both the N = 4 and N = 8 wavelets). The WM performance is depicted for only one scale (scale 10) since performance did not vary across scale. This result verifies Wornell's observations and Ptasinksi's results
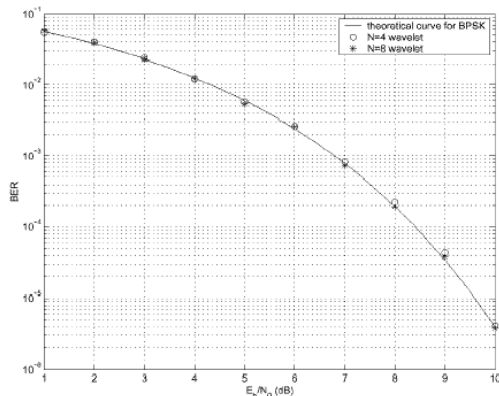

Figure 2: Bit Error Rate (BER) vs. E_b/N_0 of WM and BPSK in an AWGN channel. WM performance matches BPSK and is nearly identical for both wavelets.

Figure 3 depicts a linear BER curve inversely proportional to SNR. The curve flattens out at 35dB for demodulation at scales 10, 11 and 12; however, the curve continues to decrease at scale 13. This improvement can be attributed to the slower fading rate of the channel at scale 13 (since the bit duration decreases for increasing scale, the channel is a slower fading channel at scale 13). Figure 4 illustrates similar performance of WM at scale 13 with the theoretical performance of BPSK in a flat fading channel. At a given scale, the $f_d = 60Hz$ channel is slower fading than the $f_d = 120Hz$ channel. At high SNR in Figure 4, the BER performance of WM in the $f_d = 60Hz$ channel is slightly better than the $f_d = 120Hz$ channel.
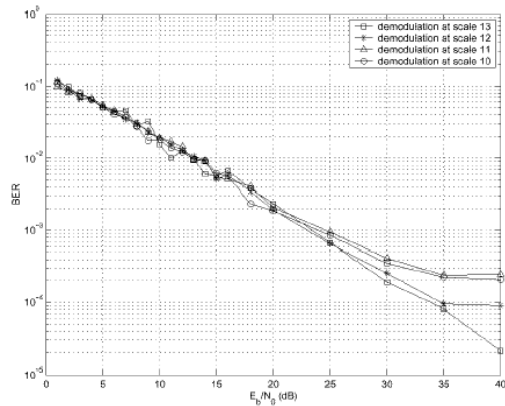

Figure 3: Bit Error Rate (BER) vs. E_b/N_0 in a flat fading channel with a doppler spread of 60Hz.
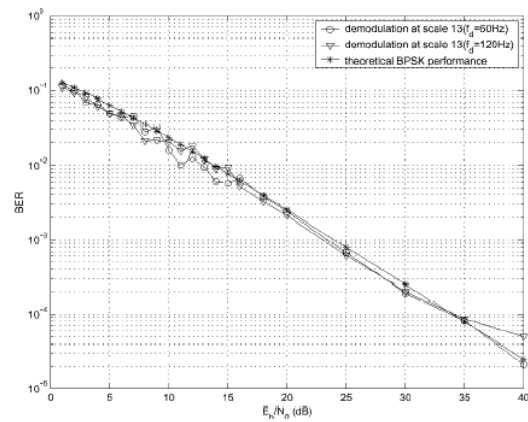

Figure 4: Bit Error Rate (BER) vs. E_b/N_0 in a flat fatling channel with doppler spreads of 60Hz and 120Hz. WM performance matches BPSK.

A difference in BER performance across scales was expected due to the frequency selective nature of the channel. Figure 5 confirms this result. At scale 13 the bit error rate is approximately 0.1 dB for all values of E_b/N_0. BER performance improves for decreasing scale: performance at scale 10 is better than the performance at scale 13. As explained earlier, the rms delay spread of $\sigma_\tau = 15,3 \mu s$ is comparable to the symbol period at scale 13 (i.e. $T_{S13} = 122 \mu s$); however, at scale 10 the symbol period, $T_{S10} = 976 \mu s$, is much larger than σ_τ. The intersymbol interference (ISI) adversely impacts scales 12 and 13, but affects scales 10 and 11 to a lesser extent. The results for the 120Hz frequency selective channel are not shown. However, the performance was similar to that of the 60Hz channel shown in Figure 5.
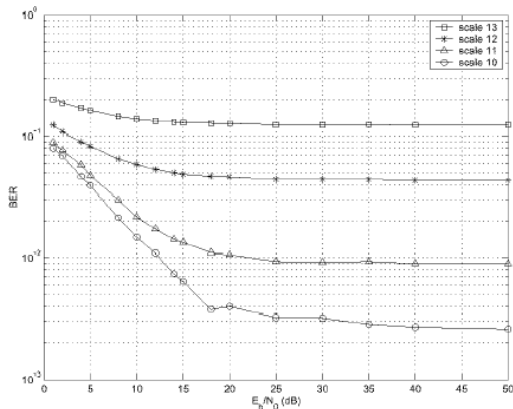
Figure 5: Bit Error Rate (BER) vs. E_b/N_0 in a frequency selective channel with f_d = 60Hz. Scale 13 is severely distorted by intersymbol interference.

Figure 6 compares the BER curve for the 3 channel types at scales 10 and 13 and f_d=60Hz (AWGN is shown only for scale 10 since all scales gave identical results). WM has the best BER performance in the AWGN channel; this is nearly identical to the BER performance of BPSK in an AWGN channel. At scale 10 (i.e. low value of ISI), the flat fading channel gives better performance than the frequency selective fading channel (for $E_b/N_0 \geq 20$).

This is due to the presence of the secondary (undesired) multipath component, which, if not in phase with the primary component will result in errors. However at scale 13, the BER performance of the flat fading channel is significantly better than the frequency selective channel for all Eb/No. At scale 13 the frequency selective channel is severely distorted by ISI.

V. CONCLUSIONS

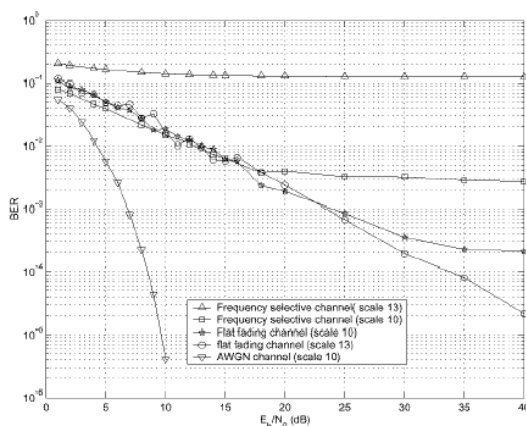There is no significant difference in WM performance for the Daubechies N = 4 and N = 8

Figure 6: Bit Error Rate (BER) vs. E_b/N_0 in the AWGN, frequency selective and flat fading channels with f_d = 60Hz. WM in the AWGN channel gives the best performance.

wavelets. WM performance in frequency selective channels is dependent on the presence of ISI; WM offers the unique advantage that if the rms delay spread is known, then the signal could be transmitted and demodulated at scales for which the IS1 is negligible. WM performance in an AWGN channel is best at all SNRs and the performance in a flat fading channel is better than a frequency selective channel. Some preliminary results with

a joint statistic that combines information at several scales indicate dramatic BER improvements: a 25dB improvement for 2 scales instead of 1 and a 6.5dB improvement for 3 scales instead of 2.

REFERENCES

[1] G. W. Word1 and A. V. Oppenheim, "Wavelet-based representations for a class of self-similar signals with application to fractal modulation," IEEE Transactions on Information Theory, vol. 38, no. 2, pp. 785 800, 1992.

[2] H. S. Ptasinski and R. D. Fellman, "Implementation and simulation of a fractal modulation communication system," Proceedings of the IEEE SUPERCOMM/ICC, vol. 3, pp. 1551-1555, 1994.

[3] I. Daubed&s, Ten Lectures on Wavelets, SIAM, Philadelphia PA, first edition, 1992.

[4] T. S. Rappaport , Wireless Communications, Prentice Hall, New Jersey, first edition, 1996.

[5] Bernard Sklar, "Rayleigh fading channels in mobile digital communication systems," IEEE Communications Magazine, pp. 90-100, 1997.